Research Article | Vol. 26, No. 13 | 25 Jun 2018 | OPTICS EXPRESS 16393
Optics EXPRESS

Nonlinear impairment scaling with the number of mode groups in mode-multiplexed transmission over a 50 µm multimode fiber

MARIUS BREHLER* AND PETER M. KRUMMRICH

TU Dortmund, Chair for High Frequency Technology, Friedrich-Wöhler-Weg 4, 44227 Dortmund, Germany
*marius.brehler@tu-dortmund.de

Abstract: We numerically investigate the impact of nonlinear effects in mode-multiplexed transmission over a 50 µm graded-index multimode fiber. Such a fiber supports 36 spatial modes, well suited for a mode-multiplexed transmission. The number of mode groups used for transmission is subsequently increased to identify the nonlinear penalty occurring due to the Kerr-effect-based nonlinear interaction between the spatial modes. It is shown that the nonlinear penalty scales less than proportional with the number of modes and hence, is no obstacle for using such a fiber for a mode-multiplexed transmission. Consequently, we clarify the potential to upgrade the transmission capacity over time with such a fiber.

OCIS codes: (060.2330) Fiber optics communications; (060.4230) Multiplexing; (060.4370) Nonlinear optics, fibers; (190.3270) Kerr effect.

References and links

1. P. J. Winzer, "Optical networking beyond WDM," IEEE Photon. J. **4**, 647–651 (2012).
2. H. R. Stuart, "Dispersive Multiplexing in Multimode Optical Fiber," Science **289**, 281–283 (2000).
3. R. Ryf, S. Randel, A. Gnauck, C. Bolle, R. Essiambre, P. Winzer, D. Peckham, A. McCurdy, and R. Lingle, "Space-division multiplexing over 10 km of three-mode fiber using coherent 6×6 MIMO processing," in Optical Fiber Communication Conference/National Fiber Optic Engineers Conference 2011, OSA Technical Digest (CD) (Optical Society of America, 2011), paper PDPB10.
4. N. K. Fontaine, R. Ryf, H. Chen, A. V. Benitez, B. Guan, R. Scott, B. Ercan, S. J. B. Yoo, L. E. Grüner-Nielsen, Y. Sun, R. Lingle, E. Antonio-Lopez, and R. Amezcua-Correa, "30x30 MIMO Transmission over 15 Spatial Modes," in *Optical Fiber Communication Conference Post Deadline Papers*, OSA Technical Digest (online) (Optical Society of America, 2015), paper Th5C.1.
5. R. Ryf, N. K. Fontaine, H. Chen, B. Guan, B. Huang, M. Esmaeelpour, A. H. Gnauck, S. Randel, S. J. B. Yoo, A. M. J. Koonen, R. Shubochkin, Y. Sun, and R. Lingle, "Mode-multiplexed transmission over conventional graded-index multimode fibers," Opt. Express **23**, 235–246 (2015).
6. J. van Weerdenburg, A. M. Velázquez-Benítez, R. G. H. v. Uden, E. Antonio-Lopez, P. Sillard, D. Molin, M. Bigot, A. Amezcua-Correa, F. Huijskens, F. Achten, H. de Waardt, T. Koonen, R. Amezcua Correa, and C. M. Okonkwo, "10 Spatial Mode Transmission over 40km 50µm Core Diameter Multimode Fiber," in *Optical Fiber Communication Conference*, OSA Technical Digest (online) (Optical Society of America, 2016), paper Th4C.3.
7. P. Sillard, D. Molin, M. Bigot-Astruc, A. Amezcua-Correa, K. de Jongh, and F. Achten, "50µm Multimode Fibers for Mode Division Multiplexing," J. Lightwave Technol. **34**, 1672–1677 (2016).
8. P. Sillard, D. Molin, M. Bigot-Astruc, A. Amezcua-Correa, K. de Jongh, and F. Achten, "DMGD-Compensated Links" in *Optical Fiber Communication Conference*, OSA Technical Digest (online) (Optical Society of America, 2017), paper Tu2J.4.
9. N. Barré, B. Denolle, P. Jian, J. Morizur, and G. Labroille, "Broadband, Mode-Selective 15-Mode Multiplexer Based on Multi-Plane Light Conversion," in *Optical Fiber Communication Conference*, OSA Technical Digest (online) (Optical Society of America, 2017), paper Th2A.7.
10. S. Bade, B. Denolle, G. Trunet, N. Riguet, P. Jian, O. Pinel, and G. Labroille, "Fabrication and Characterization of a Mode-selective 45-Mode Spatial Multiplexer based on Multi-Plane Light Conversion," in *Optical Fiber Communication Conference Postdeadline Papers*, OSA Technical Digest (online) (Optical Society of America, 2018), paper Th4B.3.
11. M. Brehler, D. Ronnenberg, and P. M. Krummrich, "Scaling of Nonlinear Effects in Multimode Fibers with the Number of Propagating Modes," in *Optical Fiber Communication Conference*, OSA Technical Digest (online) (Optical Society of America, 2016), paper W4I.3.
12. M. Brehler and P. M. Krummrich, "Impact of WDM Channel Count on Nonlinear Effects in MDM Transmission Systems," in *Optical Fiber Communication Conference*, OSA Technical Digest (online) (Optical Society of America,

#319964 https://doi.org/10.1364/OE.26.016393
Journal © 2018 Received 19 Jan 2018; revised 19 Apr 2018; accepted 21 Apr 2018; published 13 Jun 2018

Optics EXPRESS

2017), paper Th2A.63.
13. C. Antonelli, A. Mecozzi, and M. Shatif, "Scaling of inter-channel nonlinear interference noise and capacity with the number of strongly coupled modes in SDM systems," in *Optical Fiber Communication Conference*, OSA Technical Digest (online) (Optical Society of America, 2016), paper W4I.2.
14. G. Rademacher and K. Petermann, "Nonlinear Gaussian Noise Model for Multimode Fibers With Space-Division Multiplexing," J. Lightwave Technol. **34**, 2280–2287 (2016).
15. C. Antonelli, O. Golani, M. Shtaif, and A. Mecozzi, "Nonlinear interference noise in space-division multiplexed transmission through optical fibers," Opt. Express **25**, 13055–13078 (2017).
16. C. Antonelli, A. Mecozzi, and M. Shtaif, "Modeling of Nonlinear Propagation in Space-Division Multiplexed Fiber-Optic Transmission," J. Lightwave Technol. **34**, 36–54 (2016).
17. R.-J. Essiambre, M.A. Mestre, R. Ryf, A. H. Gnauck, R.W. Tkach, A. R. Chraplyvy, Y. Sun, X. Jiang, and R. Lingle, "Experimental Investigation of Inter-Modal Four-Wave Mixing in Few-Mode Fibers," IEEE Photon. Technol. Lett., **25**, 539–542 (2013).
18. A. Mecozzi, C. Antonelli, and M. Shtaif, "Coupled Manakov equations in multimode fibers with strongly coupled groups of modes," Opt. Express **20**, 23436–23441 (2012).
19. P. Sillard, "Few-Mode Fibers for Space Division Multiplexing," in *Optical Fiber Communication Conference*, OSA Technical Digest (online) (Optical Society of America, 2016), paper Th1J.1.
20. R. Schmogrow, M. Winter, M. Meyer, D. Hillerkuss, S. Wolf, B. Baeuerle, A. Ludwig, B. Nebendahl, S. Ben-Ezra, J. Meyer, M. Dreschmann, M. Huebner, J. Becker, C. Koos, W. Freude, and J. Leuthold, "Real-time Nyquist pulse generation beyond 100 Gbit/s and its relation to OFDM," Opt. Express **20**, 317–337 (2012).
21. S. Tsukamoto, K. Katoh, and K. Kikuchi, "Coherent demodulation of optical multilevel phase-shift-keying signals using homodyne detection and digital signal processing," IEEE Photon. Technol. Lett. **18**, 1131–1133 (2006).
22. M. Brehler, M. Schirwon, D. Göddeke, and P. M. Krummrich, "A GPU-Accelerated Fourth-Order Runge-Kutta in the Interaction Picture Method for the Simulation of Nonlinear Signal Propagation in Multimode Fibers," J. Lightwave Technol. **35**, 3622–3628 (2017).
23. M. Brehler and P. M. Krummrich, "Comparison of Nonlinear Impairments in Graded-Index and Trench-Assisted Graded-Index Fibers for SDM Transmissions," in *Proceedings of Photonic Networks; 18. ITG Symposium*, (VDE 2017), 77–79.
24. P. Sillard, D. Molin, M. Bigot-Astruc, K. de Jongh, and F. Achten, "Low-Differential-Mode-Group-Delay 9-LP-Mode Fiber," in *Optical Fiber Communication Conference*, OSA Technical Digest (online) (Optical Society of America, 2015), paper M2C.2.
25. W. Hermann and D. Wiechert, "Refractive index of doped and undoped PCVD bulk silica," Mat. Res. Bull. **24**, 1083–1097 (1989).
26. Y. Xiao, R.-J. Essiambre, M. Desgroseilliers, A. M. Tulino, R. Ryf, S. Mumtaz, and G. P. Agrawal, "Theory of intermodal four-wave mixing with random linear mode coupling in few-mode fibers," Opt. Express **22**, 32039–32059 (2014).
27. C. DeCusatis and I. Kaminow, *The Optical Communications Reference* (Academic, 2009).

1. Introduction

The continuous growth of traffic demand in long-haul optical transmission systems leads to capacity demands which cannot be satisfied by single-mode fibers [1]. In order to overcome the capacity of single-mode fibers, the use of spatial diversity has been proposed [2]. While most demonstrations of space-division multiplexing (SDM) systems currently consider so called few-mode fibers (FMFs), e.g. [3,4], conventional multimode fibers (MMFs) are normally used for short reach interconnects. However, the usage of conventional MMFs with graded-index profile for mode-multiplexed transmissions with 3 and 6 spatial modes over 310 km and 17 km, respectively, was reported in [5]. More recently, 10 modes were transmitted over 40 km in an MMF optimized for the transmission at 1550 nm [6]. Whereas in a FMF based experiment 15 spatial modes were utilized so far [4], MMFs with a 50 µm core diameter provide up to 8 usable mode groups with a total of 36 modes [7]. To make full use of the capacity of 50 µm MMFs in long-haul transmissions, further mode groups need to be utilized. Beside the fiber design, it is challenging to selectively excite and detect the spatial modes. Nevertheless, mode multiplexers for 15 linear polarized (LP) modes [9] are commercial available. Even a mode multiplexer for 45 Hermite-Gaussian modes was recently presented [10]. Furthermore, low complexity multiple-input multiple-output (MIMO) equalizer is needed at the receiver, leading to the requirement of small differential mode group delays (DMGD) [1]. One very promising approach to realize low DMGDs for a high number of modes, is the design of DMGD-compensated links [8]. Thus, 50 µm MMFs offer an interesting

Optics EXPRESS

option to increase the capacity of a single fiber. Still the question persists in which way the nonlinear impairments are limiting the approach to use further modes for transmission.

We investigate in which way the Kerr-nonlinearity scales with the number of utilized mode groups in our contribution. This is of interest as it clarifies in which way such a fiber link can be used initially with only a few modes for transmission, and how the transmission performance is affected when subsequently increasing the transmission capacity by utilizing further mode groups. The scaling of nonlinear impairment with the number of modes was investigated numerically for up to 15 spatial modes in [11] for a single wavelength channel. Combining mode-division multiplexing (MDM) with wavelength-division multiplexing (WDM) was numerically investigated for 15 spatial modes in [12]. We extend both and examine the nonlinear impairment, scaling with the number of used mode groups in a WDM-MDM transmission over a 50 µm MMF, by numerical simulations. In the considered scenario, up to 36 spatial modes are used for transmission over 1200 km. Several other attempts on the characterization of the nonlinear interference noise in SDM systems were reported in [13–15]. However, these models have not yet been used to analyze the nonlinear impairment for more than 10 spatial modes. To the authors' best knowledge, this is the first investigation of the scaling of nonlinear impairment for such a high number of modes.

2. Signal propagation and transmission set-up

To describe the nonlinear signal propagation we use the Manakov equation [16], which can be written as

$$\frac{\partial \mathbf{A}_{\mathfrak{a}}}{\partial z} = -\frac{\alpha}{2}\mathbf{A}_{\mathfrak{a}} - \left(\beta_{1,\mathfrak{a}} - \beta_{1,\mathrm{LP}_{01}}\right)\frac{\partial \mathbf{A}_{\mathfrak{a}}}{\partial t} - i\frac{\beta_{2,\mathfrak{a}}}{2}\frac{\partial^2 \mathbf{A}_{\mathfrak{a}}}{\partial t^2} + i\gamma\left(\kappa_{\mathfrak{a}\mathfrak{a}}|\mathbf{A}_{\mathfrak{a}}|^2 + \sum_{\mathfrak{b}\neq\mathfrak{a}}\kappa_{\mathfrak{a}\mathfrak{b}}|\mathbf{A}_{\mathfrak{b}}|^2\right)\mathbf{A}_{\mathfrak{a}}\,, \quad (1)$$

with $\mathbf{A}$ denoting the slowly varying envelopes of the mode groups $\mathfrak{a}$ and $\mathfrak{b}$. Here, α is the attenuation coefficient. The inverse group velocity is denoted by β_1, and β_2 is the group velocity dispersion (GVD) parameter. In Eq. (1), β_0 is neglected, as the phase matching condition is independent of it [17]. The Manakov equation allows accounting for different regimes of random linear mode coupling, by choosing the appropriate nonlinear coefficients κ. The calculation of the nonlinear coefficients κ is given in [16], where we do not consider Raman contributions. In our investigations, we refer to the Manakov equation for strongly coupled groups of modes [18]. The mode groups (MG) are considered as given in Table 1. According to this description, only

Table 1. Mode groups and number of spatial modes.

MG	Modes in Group								Total Number of Spatial Modes up to this MG
1	LP_{01}								1
2	LP_{11a}	LP_{11b}							3
3	LP_{02}	LP_{21a}	LP_{21b}						6
4	LP_{12a}	LP_{12b}	LP_{31a}	LP_{31b}					10
5	LP_{03}	LP_{22a}	LP_{22b}	LP_{41a}	LP_{41b}				15
6	LP_{13a}	LP_{13b}	LP_{32a}	LP_{32b}	LP_{51a}	LP_{51b}			21
7	LP_{04}	LP_{23a}	LP_{23b}	LP_{42a}	LP_{42b}	LP_{61a}	LP_{61b}		28
8	LP_{14a}	LP_{14b}	LP_{33a}	LP_{33b}	LP_{52a}	LP_{52b}	LP_{71a}	LP_{71b}	36

modes within a mode group are strongly coupled, and the inter-group coupling is assumed to be weak. This assumption is in good agreement with [19], stating that the linear coupling between the MGs weak in such a fiber, but that the modes within a mode group are strongly coupled. Since no additional mode coupling between the groups is considered, the nonlinear effects between the groups are not reduced by strong mode coupling [16]. Furthermore, intra-group modal dispersion

Optics EXPRESS

is neglected, which can lead to an additional reduction of the nonlinear impairment [15]. We leave this for future investigations. Therefore, our results define an upper boundary for the Kerr-induced nonlinear impairment.

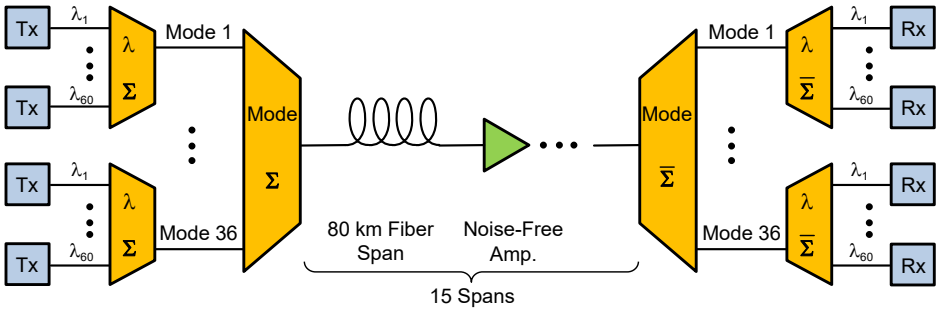

Fig. 1. Transmission set-up considered within the numerical simulations. The number of utilized MGs is varied in the simulations between 1 and 8, resulting in a minimum of a single and a maximum of 36 spatial modes used for transmission. The 60 wavelength channels per spatial mode are placed in a 50 GHz grid, and each wavelength channel carries a 32 Gbaud DP-QPSK signal.

Within the numerical simulations, we assume a transmission set-up as visualized in Fig. 1. The simulated transmission line consists of 80 km spans. With the number of spans $N_{\text{span}} = 15$, the total transmission distance is 1200 km. To compensate the span loss L_{span} of 16.8 dB, each span is followed by a noise-free amplifier with flat gain. We add noise at the end of the transmission line. Nonlinear interactions between signals and noise during propagation in the fiber are therefore not taken into account. We consider DP-QPSK modulated signals with a symbol rate of $R_s = 32$ Gbaud, and a roll-off of 0.1 for pulse shaping. Each wavelength channel is hence capable to transmit a 100 Gbit data-stream, assuming a 28 % overhead for forward error correction. Here, 60 wavelength channels are placed in a 50 GHz grid, equally around the channel at 193.4 THz corresponding to $\lambda = 1550.11$ nm, similar to [12]. With 191.95 THz as the lowest and 194.9 THz as the highest channel center frequency, a total bandwidth of 3 THz is used for transmission. This results in a total of up to 4320 spatial, polarization, and wavelength channels, each with an average launch power of P_{channel}, or rather 2160 DP-QPSK channels. The chromatic dispersion is fully compensated at the receiver. Furthermore, a clock recovery [20] and a phase recovery [21] (with Wiener filter) are used within the digital signal processing (DSP) stage. Since the linear coupling is taken into account by choosing the appropriate nonlinear coupling coefficients in Eq. (1), and since no further linear coupling is assumed, MIMO equalization is not necessary within the DSP stage. Accordingly, the signal degradation has its origin in either the noise added at the end of the transmission line or the Kerr-nonlinearity. As a performance metric, we evaluate the squared Q-factor. After applying the clock and phase recovery, the Q-factor is calculated for each polarization, and for each IQ tributary individually, and afterwards averaged over polarization and IQ tributary. To capture the impact of the nonlinear effects accurately 2^{14} symbols per spatial, polarization and wavelength channel are simulated. Each symbol is represented by 128 samples, resulting in the simulation of a spectral bandwidth of 4.096 THz. All simulations are performed using a GPU-accelerated implementation of the fourth-order Runge-Kutta in the Interaction Picture (RK4IP) method [22]. For the set-ups with 7 and 8 MGs, a modified implementation is used, capable to run a single simulation on multiple GPUs. Each simulation is executed with double precision on up to two NVIDIA Tesla K40c GPU accelerators.

Optics EXPRESS

3. 50 µm graded-index multimode fiber

The chosen graded-index fiber is closely resembling the fiber described in [7] with a core radius of 25 µm, a core-cladding index difference of $15 \cdot 10^{-3}$ at 1550 nm, and a profile exponent of 1.94. Furthermore, a trench with a width of 3.5 µm and a cladding-trench index difference of $6.5 \cdot 10^{-3}$ for 1550 nm is assumed in distance of 1.25 µm to the core. Such a fiber supports up to 10 MGs of which 8 MGs are well suited for MDM transmissions. The two highest-order MGs suffer from a too high bend loss to be utilized for MDM [7]. The effective areas A_{eff} are given in Table 2. With a nonlinear parameter $n_2 = 2.6 \cdot 10^{-20}\,\text{m}^2\,\text{W}^{-1}$, and the definition

Table 2. Effective areas of the LP modes in μm^2.

Mode	LP_{01}	$LP_{11a,b}$	LP_{02}	$LP_{21a,b}$	$LP_{12a,b}$	$LP_{31a,b}$	LP_{03}	$LP_{22a,b}$	$LP_{41a,b}$	$LP_{13a,b}$
A_{eff}	180.8	243.5	369.5	326.6	394.4	393.7	542.5	494.5	451.4	529.2
Mode	$LP_{32a,b}$	$LP_{51a,b}$	LP_{04}	$LP_{23a,b}$	$LP_{42a,b}$	$LP_{61a,b}$	$LP_{14a,b}$	$LP_{33a,b}$	$LP_{52a,b}$	$LP_{71a,b}$
A_{eff}	576.7	503.0	706.1	639.9	648.6	550.0	653.2	729.7	713.1	593.4

of $\gamma = (n_2\omega_0)/(c_0 A_{\text{eff,LP}_{01}})$, the large effective area of the fundamental mode, LP_{01}, results in a nonlinear coefficient γ of $0.58\,\text{W}^{-1}\,\text{km}^{-1}$. In the preceding definition, ω_0 specifies the center frequency of the optical signal and c_0 is the speed of light in the vacuum. As reported in [23], the exact position of the trench shows a negligible influence on the nonlinear coupling coefficients κ. However, the DMGDs can be minimized by slightly adjusting the trench position [24]. Thus, minimized DMGDs similar to [7] are assumed, as specified in Table 3. The derivatives of the

Table 3. DMGDs of the MGs in ps/km, similar to [7], and D in ps/(nm·km).

Mode Group	1	2	3	4	5	6	7	8
DMGD vs. LP_{01}	\	-47.4	-83.0	-93.9	-104.4	-119.0	-139.5	-159.1
Average D	20.1	20.3	20.5	20.6	20.8	21.0	21.2	21.6

propagation constants, and thus β_2, are derived numerically. For this purpose, the dispersion properties of the Ge-doped silica core, the F-doped silica trench, and the undoped silica cladding have been modeled using the Sellmeier equation with the coefficients provided in [25]. All modes feature dispersion parameters D between 20 and 22 ps/(nm·km), which are averaged per group and are given in Table 3.

As experimentally demonstrated in [17], inter-modal four-wave mixing can occur between the different modes in few-mode fibers. In contrast to a single-mode fiber, which needs to be operated near the zero dispersion wavelength to achieve phase matching, the phase matching condition can be fulfilled over a large frequency range due to different propagation constants of the individual modes. Hence, the phase matching condition incorporates β_1, the first derivative of the propagation constant, and thus depends on the DMGDs. For more details see e.g. [26]. Consequently, we also evaluate the case in which the DMGDs fulfill the phase matching condition for the fundamental mode, which is the worst case for the nonlinear effects. The fundamental mode is the only spatial channel which is used in all simulation set-ups for data transmission. The higher order modes are added successively, with an increase of the number of mode groups. Using Eq. (33) given in [15], we calculate the DMGDs for m=l=1 and m=1, l= − 1, respectively. Thus, all higher order modes fulfill the phase matching condition with the neighboring wavelength channel of the fundamental mode, leading to a maximal cross-group cross-phase modulation (m=l=1), later on denoted as XGXPM, and a maximal cross-group four-wave mixing (m=1, l= − 1), denoted as XGFWM. Thus, our simulations cover the two dominating four-wave mixing processes A and B [14]. The calculated DMGDs are given in Table 4. For larger DMGDs the phase matching condition can still be fulfilled, but in that case the mixing would occur with another wavelength channel.

Optics EXPRESS

Table 4. Calculated DMGDs of the MGs for maximal XGXPM and XGFWM in ps/km.

Mode Group	1	2	3	4	5	6	7	8
DMGDs, XGXPM	\	-8.14	-8.2	-8.27	-8.34	-8.42	-8.5	-8.64
DMGDs, XGFWM	\	-8.07	-8.07	-8.07	-8.07	-8.07	-8.07	-8.07

4. Simulation results and discussion

We investigate the impact of the nonlinear effects depending on the number of mode groups used for transmission within our analysis. At first, we estimate the optimal launch power per WDM channel by analyzing the squared Q-factor and identify its maximum. For this purpose, a system optical signal-to-noise ratio (OSNR), as given for instance in [27], is determined as

$$\mathrm{OSNR_{dB}} = 58 - \mathrm{NF} + P_{\mathrm{channel}} - L_{\mathrm{span}} - 10 \cdot \log_{10} N_{\mathrm{span}} \tag{2}$$

with a noise figure of NF = 5 dB. The average launch power per DP-QPSK channel is varied between −3 and 5 dBm, and the Q^2-factor is analyzed at the corresponding system OSNR. The

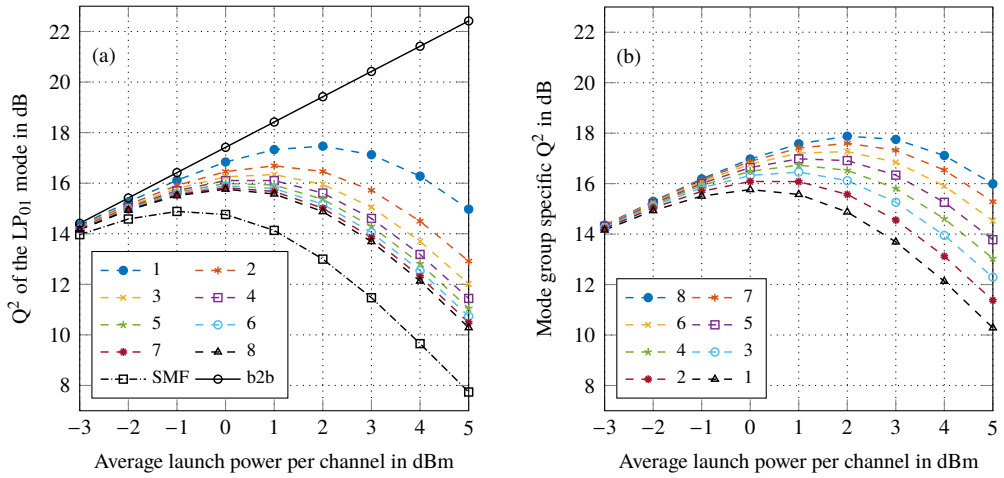

Fig. 2. Mean Q^2-factor vs. average launch power per DP-QPSK channel. (a) Different number of MGs are used for signal transmission. (b) All MGs are used for signal transmission.

mean Q^2-factor over all wavelength channels of the LP_{01} mode is shown in Fig. 2(a), whereat the number of MGs used for signal transmission is scaled up from 1 to 8. Here, DMGDs as given in Table 3 are assumed. In addition, the back-to-back (b2b) system performance is visualized in Fig. 2(a). For the case that only the first MG is used, i.e. the LP_{01} mode only, the optimal launch power is 2 dBm per DP-QPSK channel. The optimal launch power for the LP_{01} mode decreases if further MGs are utilized for signal transmission. Utilizing all 8 MGs and all 36 spatial modes, respectively, the optimal launch power for the LP_{01} mode is 0 dBm per DP-QPSK channel. Comparing the case when only the first MG is used or all 8 MGs are utilized, the maximal Q^2-factor of the LP_{01} decreases by 1.7 dB for the optimal launch powers. Thus, a nonlinear penalty clearly occurs due to making use of the higher order modes (HOM) for transmission. However, even if utilizing all MGs, the optimal launch power is 1 dB above the launch power that we identified as optimal for a single-mode fiber (SMF). For the SMF, mostly the same parameters, except for a dispersion parameter D of 17 ps/(nm·km) and a nonlinear coefficient $\gamma = 1.36\,\mathrm{W^{-1}\,km^{-1}}$, were assumed. The Q^2-factor of the fundamental mode is

Optics EXPRESS

still 0.88 dB higher for the 50 µm MMF, using all modes for transmission with a launch power of 0 dBm, compared to the SMF at the optimal launch power of −1 dBm. Assuming the identical launch power of −1 dBm for the fully utilized MMF and the SMF, the LP_{01} transmitted in the MMF still exhibits a 0.62 dB improved Q^2-factor. Thus, performance is still better than the one of a single-mode fiber while simultaneously providing a higher spatial efficiency in case of transmitting multiple MGs. The mode group specific Q^2-factors for the case that all modes are used for signal transmission are shown in Fig. 2(b). Since no significant differences within an MG are observed, the mean over all modes in an MG and over all wavelength channels is shown. The HOMs suffer from lower signal degradation and feature higher Q^2-factors, as they feature smaller nonlinear coupling coefficients κ. In contrast, the LP_{01} mode suffers from the strongest impairment, as it features the smallest effective area and the highest nonlinear coupling coefficients κ. For the 8th MG, the maximum Q^2-factor in Fig. 2(b) is about 0.4 dB above the one of the fundamental mode in Fig. 2(a), which is maximal if only the fundamental mode is utilized.

We further analyze the squared Q-factor for the launch powers of −1 and 0 dBm in more detail. In addition to the DMGDs specified in Table 3, we perform simulations for DMGDs fulfilling the phase matching condition as discussed in the previous section. The mode specific Q^2-

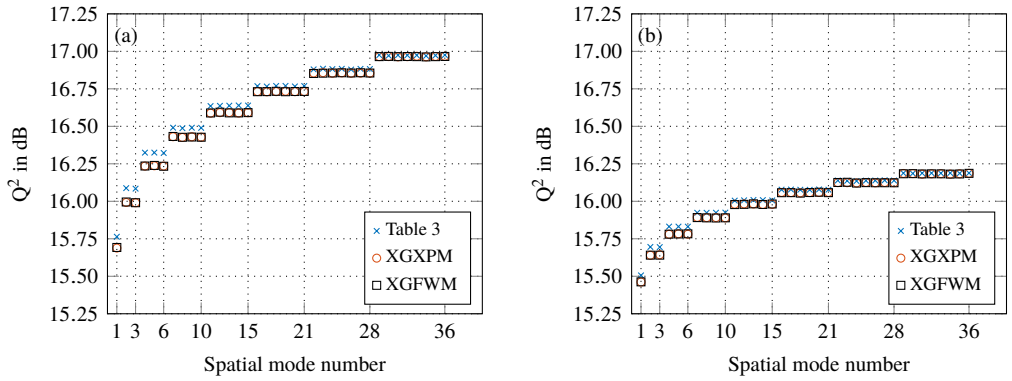

Fig. 3. Mode specific mean Q^2-factor (a) at the system OSNR of 21.44 dB and an average launch power of 0 dBm per DP-QPSK channel and (b) at the system OSNR of 20.44 dB and an average launch power of −1 dBm per DP-QPSK channel.

factors for the fully utilized MMF are shown in Fig. 3. Again, the mean is formed over all wavelength channels for a specific mode. As previously stated, the fundamental mode experiences the highest signal degradation. Furthermore, the mode groups can be clearly identified. The highest Q^2-factors can be achieved for the optimal average launch power of 0 dBm at an OSNR of 21.44 dB. However, in this scenario, the Q^2-factors show a huge, mode dependent, spread. The HOMs show an up to ∼1.21 dB improved Q^2-factor, compared to the fundamental mode. Despite the fact that more modes are propagating within the higher order MGs, the inter-group nonlinear effects do not strongly degrade their transmission performance. Although more modes propagate within each additional mode group, the increased effective areas result in smaller inter-group nonlinear coupling coefficients, leading to smaller penalties and improved Q^2-factors. As deducible from Fig. 2(b), the spread can be reduced by choosing a lower average launch power. With an average launch power set to −1 dBm, the difference between the highest and the lowest Q^2-factor decreases to 0.68 dB. Though, for a launch power of −1 dBm and an OSNR of 20.44 dB the absolute Q^2-factors are smaller. We note that in the set-ups where the DMGDs match the phase matching condition, lower Q^2-factors are obtained. However, for the long transmission distance and the moderate channel powers, the additional penalty is negligible.

Optics EXPRESS

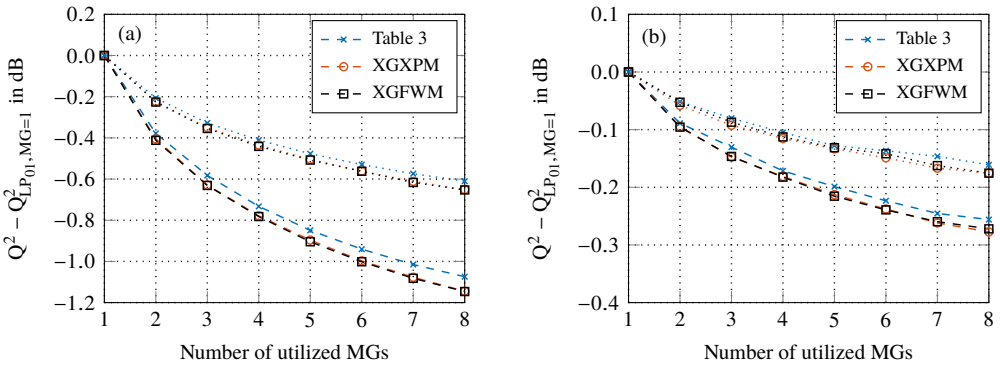

Fig. 4. Relative mean Q^2-factor of the LP_{01} mode for an average launch power of 0 dBm per DP-QPSK channel (dashed) and −1 dBm per DP-QPSK channel (dotted) at (a) the system OSNR of 21.44 dB and 20.44 dB, respectively, and (b) an OSNR of 14 dB.

Finally, the penalties for the LP_{01} mode are analyzed to clarify the scaling of the nonlinear impairments and a possible upgrade potential of such a fiber. Utilizing further MGs for transmission results in a penalty of < 1.2 dB for an average launch power of 0 dBm at an OSNR of 21.44 dB, and < 0.66 dB for a launch power of −1 dBm and an OSNR of 20.44 dB, as shown in Fig. 4(a). Again, only a small additional penalty occurs if the phase matching condition is fulfilled. We note that in the so far performed analysis rather high OSNRs were assumed. Therefore, the nonlinear effects are the dominating origin of signal degradation. Considering a lower OSNR, the penalty decreases considerably as shown in Fig. 4(b) for an OSNR of 14 dB. Increasing the noise level at the receiver, the penalty is below 0.3 dB.

Our results show that the Kerr-induced nonlinear impairment does not prohibit the use of a 50 µm MMF for MDM transmission. Most importantly, considering the nonlinear impairments, one can start with only using the fundamental mode for transmission and easily increase capacity by utilizing further MGs without strongly degrading the lower order modes.

5. Conclusions

We have investigated the impact of nonlinear effects for a wavelength-division and mode-division multiplexed transmission over 1200 km of a 50 µm graded-index multimode fiber by numerical simulations. The number of mode groups and spatial modes, respectively, used for transmission was increased, and the influence on the squared Q-factor was analyzed. Scaling the number of utilized modes up to 36, the optimal launch power per DP-QPSK channel for the fundamental mode is decreased from 2 dBm to 0 dBm. Transmitting only the fundamental mode or utilizing all 36 modes leads to a decrease of the squared Q-factor by 0.3 dB for the optimal launch power and an OSNR of 14 dB. Penalties occurring due to a fulfilled phase matching condition could be observed, but are negligibly small. The Kerr-effect-based nonlinear interactions between the modes do not seem to prohibit the usage of 50 µm graded-index fibers as a transmission medium for mode-multiplexed systems. Furthermore, such a fiber provides the potential to be deployed and to initially only use a few modes for transmission. Upgrading the capacity by utilizing further modes capable of propagation does not strongly affect the transmission performance, since the induced nonlinear impairments scale less than proportional with the number of modes.

Optics EXPRESS

Funding

Deutsche Forschungsgemeinschaft and Technische Universität Dortmund/TU Dortmund Technical University within the funding programme Open Access Publishing

Acknowledgments

The authors are grateful for the donation of a Tesla K40c GPU by NVIDIA through the GPU Grant program, used for this research. We acknowledge financial support by Deutsche Forschungsgemeinschaft and Technische Universität Dortmund/TU Dortmund Technical University within the funding programme Open Access Publishing.